FINAL REPORT

PILOT STUDY: POLYGRAPH DECISION SUPPORT SYSTEM USING EVENT RESOLUTION IMAGING FOR THE RELEVANT/IRRELEVANT FORMAT

February 19, 2003

Daniel R. Cook, Richard F. Kennard, Jeremy P. Almond

Thoughtform Corporation
85 West 400 North
Bountiful, UT 84010

Corresponding author and Principle Investigator:

Daniel R. Cook, Ph.D.
Thoughtform Corporation
85 West 400 North
Bountiful, UT 84010
Tel: (801) 299-1285
Fax: (801) 292-7217
Email: dan@thoughtform.com

REPORT DOCUMENTATION PAGE

Public reporting burden for this collection of information is estimated to average 1 hour per response, including the time for reviewing instructions, searching existing data sources, gathering and maintaining the data needed, and completing and reviewing the collection of information. Send comments regarding this burden estimate or any other aspect of this collection of information, including suggestions for reducing this burden, to Washington Headquarters Services, Directorate for Information Operations and Reports, 1215 Jefferson Davis Highway, Suite 1204, Arlington, VA 22202-4302, and to the Office of Management and Budget, Paperwork Reduction Project (0704-0188), Washington, DC 20503.

1. AGENCY USE ONLY *(Leave blank)*	2. REPORT DATE February 19, 2003	3. REPORT TYPE AND DATES COVERED September 15, 2000 - September 14, 2001

4. TITLE AND SUBTITLE
Pilot Study: Polygraph Decision Support System Using Event Resolution Imaging for the Relevant/Irrelevant Format

5. FUNDING NUMBERS
DoDPI99-P-0006

6. AUTHOR(S)
Daniel R. Cook, Richard F. Kennard, and Jeremy P. Almond

7. PERFORMING ORGANIZATION NAME(S) AND ADDRESS(ES)
Thoughtform Corporation
85 West 400 North
Bountiful, UT 84010

8. PERFORMING ORGANIZATION REPORT NUMBER

9. SPONSORING / MONITORING AGENCY NAME(S) AND ADDRESS(ES)
DoD Polygraph Institute
7540 Pickens Avenue
Fort Jackson, South Carolina 29207

10. SPONSORING / MONITORING AGENCY REPORT NUMBER
DoDPI02-R-0003

11. SUPPLEMENTARY NOTES

12a. DISTRIBUTION / AVAILABILITY STATEMENT
Unlimited Distribution

12b. DISTRIBUTION CODE

13. ABSTRACT *(Maximum 200 words)*

A mathematical and statistical signal processing strategy, termed Event Resolution Imaging (ERI), was applied to the problem of developing a new polygraph decision support system for the Relevant/Irrelevant question format. The Event Resolution Imaging (ERI) methodology was employed to analyze and separate raw polygraph signals into truthful and deceptive categories. By extracting the traditional point features of respiratory waveform length, cardiovascular baseline amplitude and EDR amplitude, along with the signal features of distinct frequencies, latencies, amplitudes and phase correlations, a relatively high accuracy has been achieved. Scoring protocols were designed using data from 577 polygraph examinations for which examinee veracity was known. The optimal scoring protocol was cross-validated using 144 polygraph examinations for which examinee veracity was not known. The veracity of examinee responses to the question "Have you smoked marijuana in the last 30 days?" was correctly identified for 109 (i.e., 76%) of the 144 cases. This accuracy was 13% higher that that achieved by a commercial scoring algorithm and 6% higher than the estimated accuracies achieved by human experts.

14. SUBJECT TERMS		15. NUMBER OF PAGES 34
		16. PRICE CODE

17. SECURITY CLASSIFICATION OF REPORT U	18. SECURITY CLASSIFICATION OF THIS PAGE U	19. SECURITY CLASSIFICATION OF ABSTRACT U	20. LIMITATION OF ABSTRACT U

TABLE OF CONTENTS

Listing of Figures

1.0   ABSTRACT

A mathematical and statistical signal processing strategy, termed Event Resolution Imaging (ERI), was applied to the problem of developing a new polygraph decision support system for the Relevant/Irrelevant question format. The Event Resolution Imaging (ERI) methodology was employed to analyze and separate raw polygraph signals into truthful and deceptive categories. By extracting the traditional point features of respiratory waveform length, cardiovascular baseline amplitude and EDR amplitude, along with the signal features of distinct frequencies, latencies, amplitudes and phase correlations, a relatively high accuracy has been achieved. Scoring protocols were designed using data from 577 polygraph examinations for which examinee veracity was known. The optimal scoring protocol was cross-validated using 144 polygraph examinations for which examinee veracity was not known. The veracity of examinee responses to the question "Have you smoked marijuana in the last 30 days?" was correctly identified for 109 (i.e., 76%) of the 144 cases. This accuracy was 13% higher that that achieved by a commercial scoring algorithm and 6% higher than the estimated accuracies achieved by human experts.

2.0   INTRODUCTION

There is a need to increase the validity, reliability, and accuracy of PDD examinations using the Relevant/Irrelevant (R/I) Test Format. There is also a need to better understand and automate the process of determining whether a subject is being truthful or deceptive during a polygraph examination. The development of improved computer algorithms, which accurately process polygraph waveforms to better determine deception or truthfulness, will benefit the field of forensic psychophysiology.

Our research seeks to benefit the field of personnel security by improving the accuracy and reliability of PDD examinations by adaptively combining information from the standard polygraph channels of respiration, electrodermal response, and cardiovascular activity. Improving the accuracy and reliability of PDD examinations will enhance personnel security in the Department of Defense, the Armed Forces and in the civilian workplace where personnel security is an issue.

Standard polygraph data for the detection of deception in verbal communication consists of four waveform channels of physiological responses: electrodermal, cardiovascular, and respiratory responses. Polygraph data has traditionally been analyzed and evaluated by a trained polygraph examiner. The polygraph examiner visually inspects and compares the polygraph waveform responses evoked by various questions. Typical questions include irrelevant questions, comparison questions and relevant questions (Abrams, 1989). The relevant questions deal directly with the issue being investigated. The comparison questions deal with issues that are similar to, but not related to, the issue at hand. The irrelevant questions concern neutral issues that are unlikely to evoke any emotional arousal.

The Comparison Question Test is among the most common of polygraph tests. It evaluates whether the subject has a larger physiological response to comparison questions or relevant questions. The premise is that innocent subjects will experience greater concern and emotional

arousal when presented with a comparison question than when presented with a relevant question, and that guilty subjects will experience greater concern and emotional arousal when asked relevant questions that deal with the particular issue in question. The polygraph examiner compares a subject's reaction to a relevant question with the subject's reaction to a comparison question that has been carefully prepared and coupled with the relevant question. The examiner then determines which physiological response represents a larger level of emotional arousal. The examiner also decides what degree of significance to attach to the observed differences in evoked physiological waveforms. Each chart of polygraph recordings consists of at least two comparison-relevant question pairs. The examiner records and compares responses from at least two charts per examination. The polygraph examiner considers all available information and makes a determination as to whether the subject is being deceptive or non-deceptive.

Like other polygraph testing techniques, the R/I Test Format is based on the belief that, with proper pretest interviewing, test question structure, and sequencing, an involuntary psychophysiological reaction will occur when an examinee is asked a specific question about an issue that is important to his or her well being and to which that person is deceptive. This psychophysiological reaction will be distinguishable from the examinee's norm taking into consideration the excitement level of the situational setting.

While a skilled and experienced polygraph examiner can achieve impressive results, human visual inspection of waveforms is notoriously fraught with potential for observer error. Human visual inspection may also miss subtle changes in the waveforms themselves, including relationships between individual waveform channels, which may be significant.

The study of the use of computers in Psychophysiological Detection of Deception (PDD) Tests has progressed through several phases since 1962 (Yankee, 1995). During the first phase, several potential computer applications were considered (Kubis, 1962; Yankee, 1968; Burch, 1969). In the second phase, researchers used various methods to evaluate physiological data collected with laboratory or traditional polygraphs (McGuigan, 1972; Podlesny, 1976; James, 1982; Kircher & Raskin, 1988; Raskin et al., 1988; Honts, 1986; Giles & Yankee, 1986; Timm, 1989). During this time, the first Computer Assisted Polygraph System (CAPS) was developed incorporating the first algorithm to be used for diagnostic purposes (Kircher & Raskin, 1989). The current phase of development has produced three American computerized polygraphs that stand alone without the need for interfacing with traditional or laboratory polygraphs. These three systems are the Axciton (Axciton Systems, Inc.), the Computerized Polygraph System or CPS (Stoelting) and the Lafayette (Layfayette Instruments). Each of these systems comes with its own hardware and software. A major advantage of computerized polygraph systems over traditional polygraph systems is that the analog physiological signals are transformed into digital signals necessary for the development of automatic polygraph scoring algorithms.

Most polygraphs used in PDD testing continue to collect cardiovascular, electrodermal and respiratory information with the same sensors and transducers that have been in use for over fifty years. However, computer algorithms are now able to analyze physiological responses to test questions and estimate the probability that the questions were answered correctly. The algorithm developed by Kircher and Raskin (Kircher & Raskin, 1988,1989) is used with the CAPS and the

CPS. Its diagnostic capability is limited to Comparison Question Tests. CAPS and CPS have been used by field PDD examiners, including the U.S. Secret Service, for more than a decade.

In 1993 the Applied Physics Laboratory at John Hopkins University completed an algorithm to score zone-comparison question tests from PDD field test data collected on Axciton computerized polygraphs. The Polygraph Automated Scoring System (PASS) software was developed and then replaced by a software package called Polyscore, which uses a sophisticated mathematical algorithm to analyze the data and estimate a probability or degree of deception or truthfulness. The database used to develop the Polyscore 2.3 software was established by using 539 PDD field criminal examinations.

The two major automated scoring algorithms currently in use appear to be the CPS and the Polyscore algorithms. Various tests have been conducted to determine the level of accuracy of these algorithms. It appears that these algorithms can often achieve high accuracy rates and are, in some ways, about as accurate as human examiners using visual inspection. However, human visual inspection is still considered, by most polygraph examiners, to be the most reliable method of scoring polygraph data charts. Computer algorithms are currently used to provide a back-up, or second opinion, on data that is visually scored by a human expert. This may continue to be the case until algorithms can be developed that reliably surpass human evaluation capabilities.

In the future, new types of human physiological data, such as systolic time intervals and raw (non-averaged) electroencephalogram, may be used in some PDD exams. These new types of physiological signals might be very difficult for human examiners to visually score. In such cases, the use of computer algorithms may be the only way to obtain an accurate diagnosis. However, since the use of computer algorithms in PDD examinations is still in its developmental stages, it is important to proceed with caution and to carefully evaluate every new advance in order to appropriately determine the degree of reliance that one can place on any computer algorithm.

A number of advanced analysis methods have been applied to electroencephalographic (EEG) and magnetoencephalographic (MEG) signals which may be successfully applied to the analysis of physiological polygraph data, especially if they are able to make use of inter-channel relationship information and can feasibly be integrated with computerized condition discrimination.

Many methods can provide sophisticated analyses of individual waveform information channels independent of computerized condition discrimination. These methods include Fourier Transforms (Scherg et al., 1989), Hilbert Transforms (Witte et al., 1990), Wavelet Transforms (Bertrand et al., 1994), Short-Time Fourier Transforms (Makeig, 1993), Wigner Functions (Cook et al., 1993), Generalized Time-Frequency Distributions, and other joint Time-Frequency Distributions. These transforms are very valuable for their various indications. However, they are usually done using only a single channel, and inter-channel relationships are often missed. Also, until now, these methods have not been integrated with computerized condition discrimination. Like spectral analysis techniques, these methods have had to rely on human visual inspection of waveforms, a process fraught with potential for observer error.

Other methods of waveform analysis are better suited to analyze multiple channels of waveform information. Many spatial filtering methods (Nunez, 1988) have been investigated with physiological data, including Principal Component Analysis, Singular Value Decomposition, and Eigenvalue Analysis (Golub, & Van Loan, 1989; Horn, & Johnson 1985; Chapman, & McCrary, 1995; Achim, & Marcantoni, 1997; Wood, & McCarthy, 1984). Various source localization methods (Scherg, 1990; Scherg, & Berg, 1991; Scherg, 1992; Cardenas et al., 1995) have been applied to estimate the locations of important electrical activity within the brain (Scherg, & Ebersole, 1993; Fuchs et al., 1995; Nunez, 1986; Turetsky et al., 1990; Zhang, & Jewett, 1993; Zhang et al., 1994; Buchner et al., 1994; Ebersole, 1991). While powerful for spatial source localization, these techniques tend to ignore frequency and temporal information. These spatial analysis methods must be applied to averaged evoked potentials or the noise level is prohibitive. Therefore, they are of limited use for single-trial (single response) analysis.

Finally, newer techniques, which take advantage of recent increases in computer processing power, have been developed. Neural networks have been created to discover discriminant information. Fuzzy logic systems have been applied to represent approximate knowledge and make robust decisions in the presence of significant uncertainty and high noise levels (Kosko, 1992). Integrated neurofuzzy systems have also been developed to combine the learning capabilities of neural networks (mostly back-propagation of errors through the net) with approximate expert knowledge represented in fuzzy If-Then rules (Kosko, 1992). Various adaptation and optimization approaches (Haykin, 1991), including Genetic Algorithms and other generation and selection methods (Carpenter, & Grossberg, 1991) are used to maximize particular processes of interest to satisfy the aim at hand. Statistical, chaotic, and other characteristic measures have been applied in the study of neurophysiological time-series data, including calculations of embedding dimensions, Liapunov exponents, fractal dimensions, interpolations, derivations, correlations, covariance, coherency, and other statistical measures (Ingber, 1995). While sometimes quite effective at determining important relationships among multiple physiological data channels, traditional neural network approaches generally take a long time to program and learn, and are difficult to train. Most of these approaches are limited by a lack of integration with time, frequency and spatial analysis techniques.

The forgoing methods of wave signal processing have provided useful concepts and are each valuable in their particular area of focus. However, due to their inherent narrow ranges of applicability, prior methods have provided a fragmentary approach to physiological signal evaluation. Because these methods all have significant weaknesses and limitations, there is a need for an integrated approach that will provide rapid and accurate analysis of all pertinent waveform characteristics of a wide variety of raw physiological waveforms. An integrated waveform analysis method that could combine the strengths and avoid the weaknesses of current methods would be an extremely valuable addition to the field of physiological detection of deception. There is a need for a computerized method of waveform analysis which can be used to simultaneously evaluate and adaptively combine multiple channels of complex waveform data stemming from distinct physiological time-series including EDR, cardiovascular, and respiratory measures.

A new integrated waveform-investigation method has been recently developed and used, which is called Event Resolution Imaging (ERI), to obtain exciting breakthrough single-trial analysis

results on EEG and MEG data sets. In particular, a new computerized analysis technique has been used to obtain robust classification results of greater than 90% accuracy on single MEG somatosensory evoked trials (Cook et al., 2001), 98% accuracy on single EEG visual evoked trials (Cook et al., 2001), 92% accuracy on single EEG motor evoked trials (Short et al., 2001), and 90% accuracy on few-trial averages of cognitive event related P300 Signals (Cook et al., 2001).

This computerized analysis technique (ERI) has also been used to develop a drug evaluation system that is able to generate blood-brain barrier crossing profiles to determine at what dosage a pharmaceutical test compound actively modifies underlying patterns in brain EEG activity. This method has also been used to show that each neurologically active compound induces a unique physiological pattern or fingerprint in the EEG, such that EEG analysis can be used to uniquely identify which of several drugs has been taken and currently exists in the brain (Steffensen et al., 2001).

This integrated waveform analysis technique (ERI) has been embedded within a new software package called the *Thoughtform Interpretation Studio* (Version 3.0 Copyright © Thoughtform Corporation, 1998-2002). This software package applies computerized condition analysis to simultaneously evaluate and adaptively combine multiple channels of complex waveform data stemming from distinct types of physiological time-series.

This new technique is highly accurate and reliable for single-trial analysis (single response) classification of MEG and EEG datasets. These algorithms may be usefully adapted and applied to other types of physiological signals, such as polygraph data. There may be a powerful application of this computerized interpretation approach to standard physiological time-series including EDR, cardiovascular, and respiratory measures.

This pilot investigation was designed to evaluate the use of the ERI approach, which was successful with EEG and MEG data, on traditional polygraph data. It was hypothesized that the ERI technique can be used to obtain an accuracy of 80% (better than that obtainable by human experts) on a set of subjects whose veracity is unknown to the experimenters.

3.0   MATERIALS AND METHODS

3.1   Data Collection:

Polygraph data for 721 examinations collected using the Relevant/Irrelevant question procedure was obtained, in ASCII format, from the Department of Defense Polygraph Institute confirmed case database. Examinee veracity was supplied for 577 examinations (396 truthful and 181 deceptive). Examinee veracity was not supplied, by agreement, for 144 of the examinations-which were to be used for cross validation.

3.2   Data Translation:

The Thoughtform ASCII translator was used to translate the ASCII polygraph data into Thoughtform Standard Format (TSF) version 1.0. ASCII is data that is shown in a text format. The data received from the DODPI was 4 columns of numbers, one for each of the physiological channels thoracic respiration, abdominal respiration, EDR, and cardiovascular, with each number

being a sample taken at 60 Hz intervals. Prior to this translation, we used a global search and replace operation to replace the question onset indicators and the response indicators in the ASCII data files with numerical values that could be read by our ASCII translator as a separate channel, called the question and answer event channel. There were also other channels containing important information: the date the examination was given, the examiner number, and the subject's veracity. The product of this process was a file in TFStudio format consisting of nine channels, including the four physiological signal channels and two question-answer event channels. There were a total of 1,908 files (6 files were rejected due to artifacts), which have thus been translated into nine-channel TSF 1.0 files. Each binary TSF file corresponded to one chart. Each chart lasted approximately five to six minutes. For simplicity in showing the process that was used to interpret the data, a series of figures (**Figures 1 and 2**) have been included. These figures are from 2 subjects (1 truthful and 1 deceptive) and illustrate the steps that were used with all of the subjects.

FIGURE 1
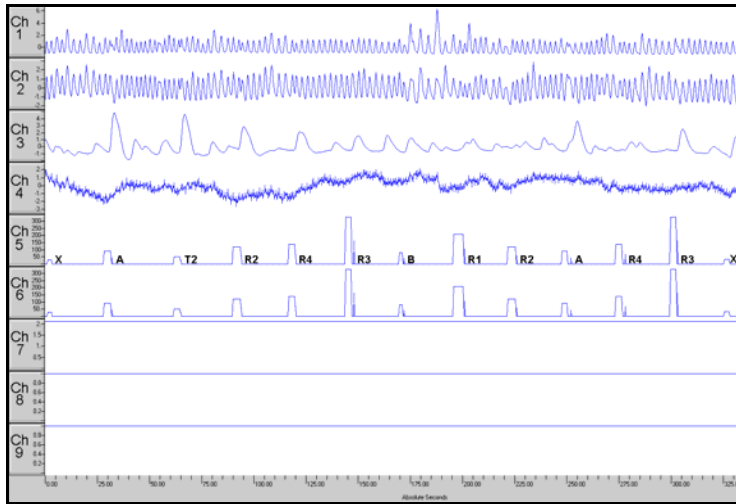
A. Truthful   **B.** Deceptive
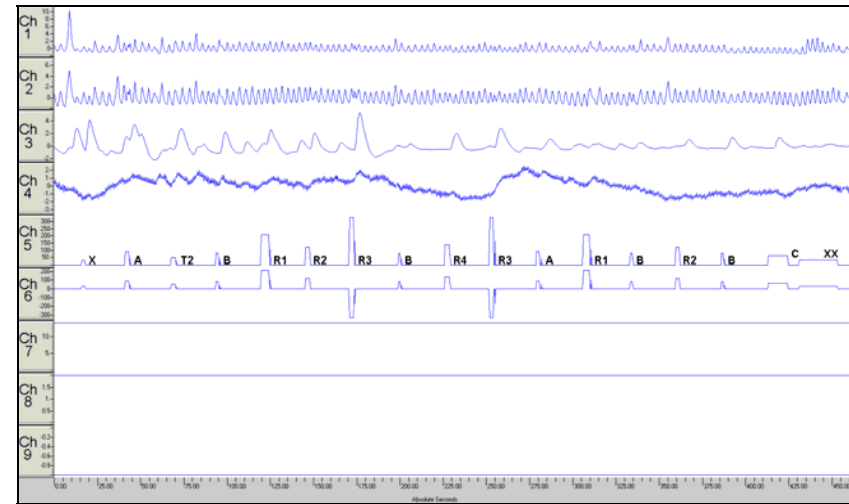
Figure 1. Raw Waves from Single Subjects: Depicts the raw PDD waves as displayed in TFStudio. The waves in **Figure 1A** are from the chart of a truthful subject, and the waves in **Figure 1B** are from the chart of a subject that was deceptive to the R3 question. Channels 1 and 2 are the respiration channels (thoracic and abdominal respectively). Channel 3 is the EDR channel. Channel 4 is the cardiovascular channel. The other channels are label channels that have been inserted by the researchers. Channels 5 and 6 show the time of question onset, duration, and offset as well as the time for the answer. The only difference between the channels is that channel 6 shows values that go down to show when the subject is deceptive to a particular question. Channel 7 shows the date that the examination was given. Channel 8 represents the examiner that administered the exam. Channel 9 shows the subjects veracity, 1.0 representing truthful and -1.0 representing deceptive.

3.3   Data Preparation

3.3.1   Artifact Rejection:

The data were visually inspected to remove from consideration epochs containing artifacts. Artifacts were defined as any noise or other influence that could contaminate the physiological signal of interest. These artifacts can be caused by many outside influences including errors in the recording apparatus, different settings used when recording the data, as well as unrecorded and unrelated physiological stimuli. Essentially, all epochs that looked significantly different from the norm were removed prior to using the learning algorithm. This artifact rejection was done manually using a utility in which epochs containing artifacts were simply not selected for further consideration by the learning algorithm.

3.3.2   Signal Preprocessing:

In order to make sure that each subject was comparable to each of the other subjects, several things were done to process the data. First, decreasing trends had to be removed from all of the charts. Second, differences in baseline amplitude between charts had to be equalized. Third, differences in variance between charts had to be equalized.

In some of the Polygraph charts there was a decreasing trend in both of the respiration channels and the cardiovascular channel. This cause of the trend is unknown, but was found to be interfering with the creation of the algorithm. Therefore, in order to remove the trend, a windowed average was taken of every file with the window being 83 seconds. This average was then subtracted from each frame in the file to produce a new chart that didn't have a trend.

A difference in the baseline amplitude between subjects, and even between charts, was decreasing the learning algorithm's accuracy. This difference could be caused by variations between examination instruments or variations between subjects. There did not appear to be a correlation between the amplitude difference and deception. The baseline difference was equalized using the *Thoughtform Interpretation Studio* software. The baseline was set for 0 on all charts.

There was also a difference in the variance of polygraph signals between charts as well as between subjects. This difference may also be based on variations between examination instruments or variations between subjects. There did not appear to be a correlation between the variance difference and deception. Because this difference was decreasing the accuracy of the learning algorithms, it was removed. The variance was set to one on a chart-by-chart basis.

3.3.3   Data Segmentation:

There were three types of events in the polygraph data to which physiological signal responses may be time-locked. They were: (1) time of question onset, (2) time of question completion and (3) time or instant in which the answer is given. All answers were very brief and correspond to either a "Yes" or a "No". Typical question durations were from 2-5 seconds. The most valuable event is the time of question onset. Epoch segments of polygraph data were extracted relative to the events of interest. An epoch was a data segment beginning at question onset and ending 25 seconds later.

FIGURE 2

A. Truthful
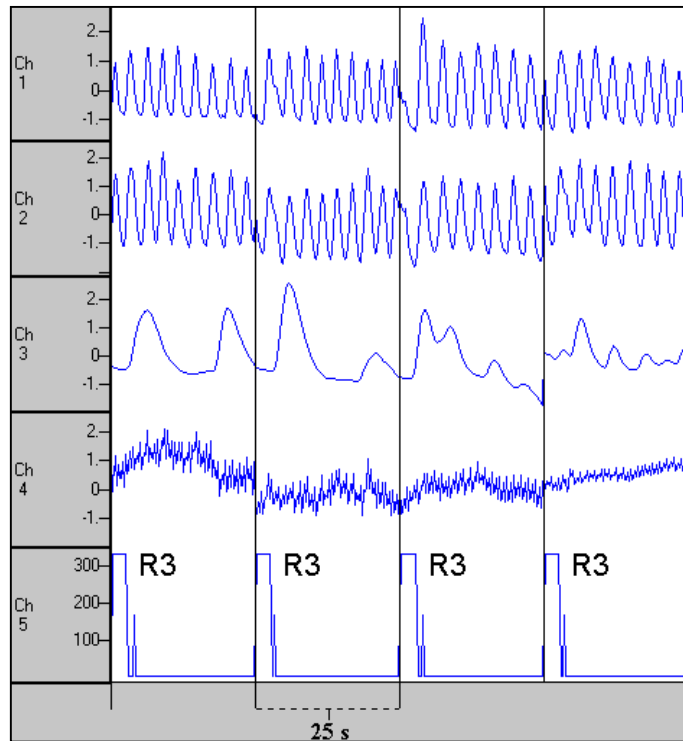
B. Deceptive
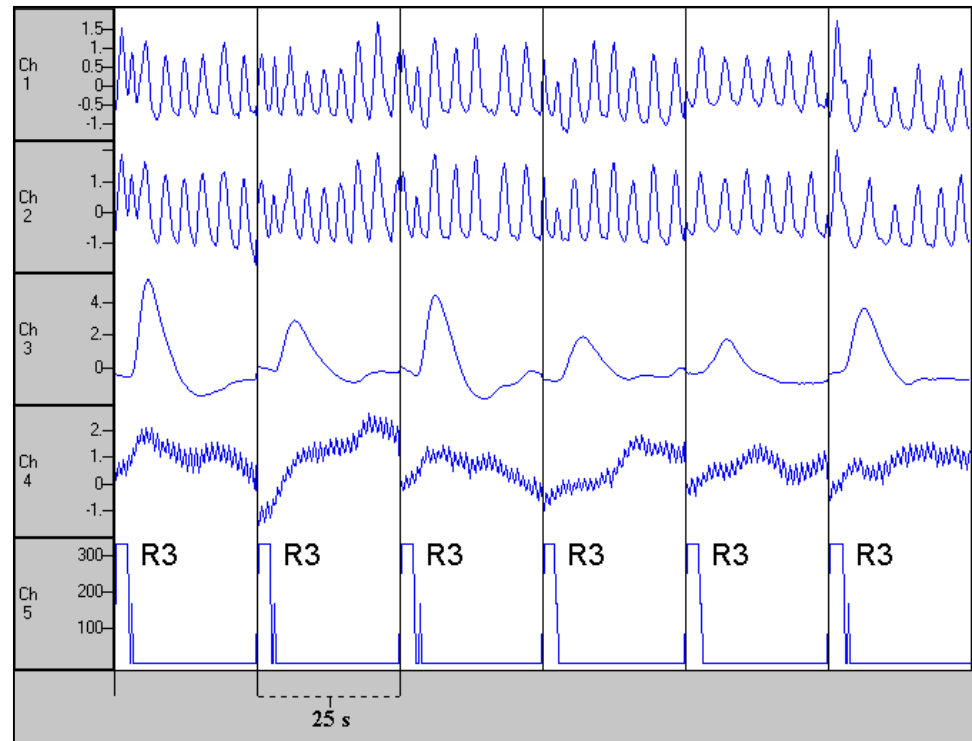
Figure 2. Raw Waves from Multiple Charts: Depicts the raw PDD waves that have been time locked to the beginning of the analysis epoch in preparation for the learning algorithm. The waves in **Figure 2A** are from a truthful subject, and the waves in **Figure 2B** are from a subject that was deceptive to the R3 question. The channels are the same as described in the **Figure 1** description, except the label channels have been removed.
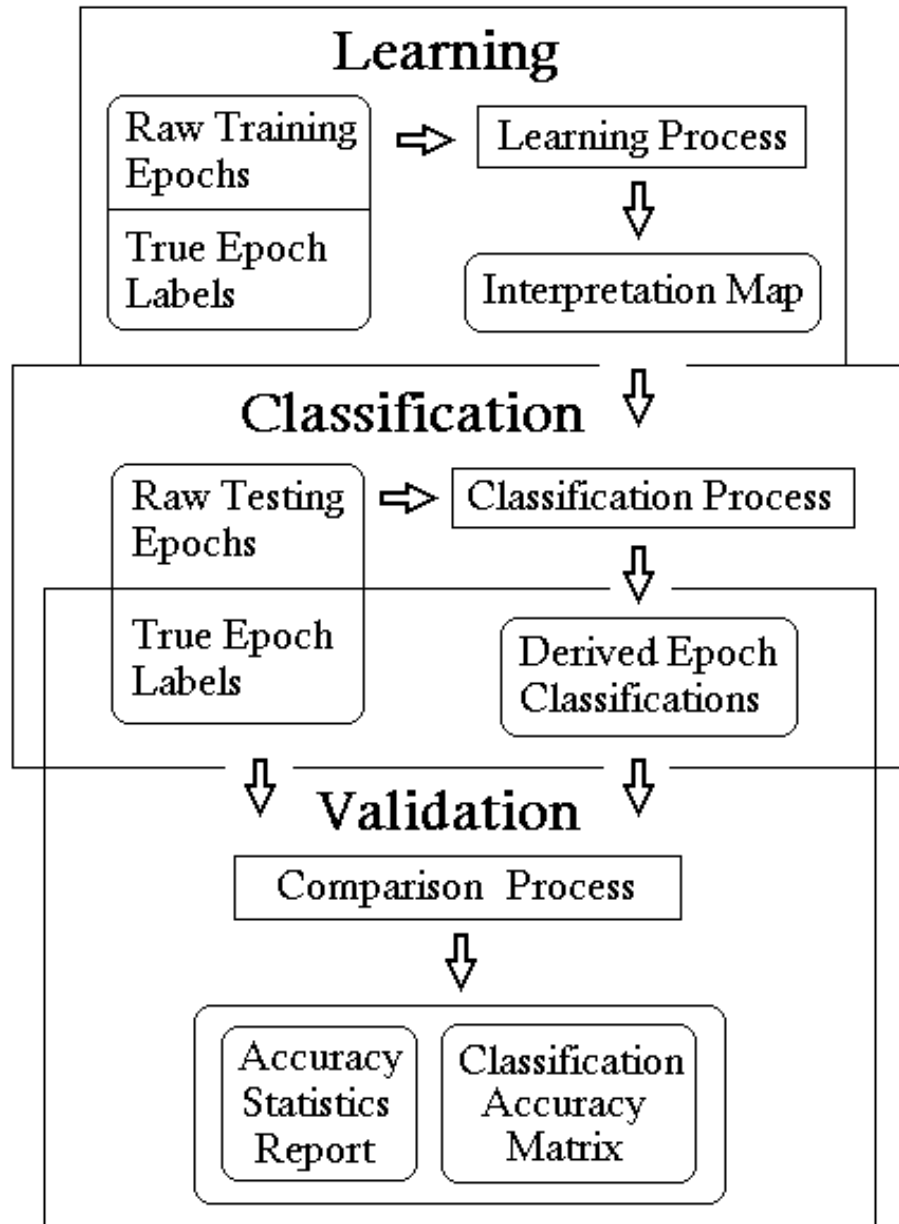
3.4   Event Resolution Imaging:

After having processed the individual PDD charts as described above, the individual events, which were time-locked to question onset into individual analysis epochs, were combined together according to whether the subjects were deceptive or non-deceptive. These PDD epochs were analyzed using Event Resolution Imaging (ERI) with the *Thoughtform Interpretation Studio* on Pentium-type computers. The basic strategy of ERI is to apply several methods of analysis to each PDD epoch to find consistent differences between PDD epoch types and similarities within the same epoch type. A flow-chart for the ERI operation is shown in **Figure 3**. ERI analysis consists of three primary processes: learning, classification, and validation. The learning process involves the following techniques for waveform analysis: time-frequency expansion, feature coherence analysis, difference component analysis, and separation analysis. Each PDD epoch is decomposed into features in an extended phase space representing spatial, time, frequency, phase and interchannel relationships (**Figure 3**). These features are then analyzed in detail for characteristics common to the epoch type. This analysis includes evaluation of coherence between signals distributed across the four domains of space, time, frequency, and phase. The *Thoughtform Interpretation Studio* next performs a set of analyses to find features that are most reliably different between epoch types, called state discriminant analysis. This consists of waveform analysis, distribution function analysis, and discriminant optimization. Finally, the results of the above analyses are used to generate a set of parameters, components, functions, and criteria, which best identifies epoch type and discriminates between epochs. This is recorded as an interpretation map wherein the ERI algorithm analyzes all factors and identifies a set of characteristics that best differentiates and identifies the epoch types. The "*interpretation map*" is then used to analyze waveforms in epochs of data which the algorithm has not previously seen (**Figure 3**).

A statistical summary of results is also generated, including the confidence level that each epoch was classified correctly, as well as calculations of sensitivity, specificity, and overall accuracy (**Figure 3**). True epoch labels (actual deceptive or non-deceptive states) are associated with raw testing epochs to enable a comparison with derived epoch classifications (predicted deceptive or non-deceptive states) generated by the classification process. The comparison process tests the equivalency of true labels and derived classifications to generate an epoch classification accuracy statistic report. A corresponding classification matrix representing the fraction of epochs of each true epoch type, which are classified as belonging to each of the classified epoch types, is also generated. High classification accuracy, on testing epochs that are separate and distinct from the training epochs used for learning, indicates a valid derived interpretation map.

FIGURE 3

Single Trial Event Resolution

Figure 3. Flow Chart of Event Resolution Imaging: Event Resolution Imaging consists of three primary processes called learning, classification, and validation.

Learning
The learning process involves the following techniques for waveform analysis: time-frequency expansion, feature coherence analysis, and principal component analysis. After epochs have been uniformly pre-processed to remove artifacts, each epoch is decomposed into features in an extended phase space representing spatial, time, frequency, phase, and interchannel relationships. These features are then analyzed in detail for characteristics common to the epoch type. This analysis includes evaluation of coherence between signals distributed in complex fashion across all four domains of space, time, frequency, and phase. The *Thoughtform Interpretation Studio* then performs a set of analyses to find features that are most reliably different between epoch types, called state discriminant analysis. This consists of waveform analysis, distribution function analysis, fuzzy logic analysis, and discriminant optimization. Finally, the results of the above analyses are used to generate a set of parameters, components, functions, and criteria, which best identifies epoch type and discriminates between epochs. This is recorded as an interpretation map. The *Thoughtform Interpretation Studio* then uses the interpretation map to apply the set of analyses and criteria it previously determined was optimal to the "unknown" epoch's classification.

Classification
The software analyzes each epoch as an individual event (no averaging) and presents it as a composite, "clean" waveform made up of those characteristics used in its analysis and classification. The *Thoughtform Interpretation Studio* also provides a statistical summary of results, including the confidence level that each epoch was classified correctly, as well as calculations of sensitivity, specificity, and validation overall accuracy.

Validation
True epoch labels may be associated with raw testing epochs to enable a comparison with derived epoch classifications generated by the classification process. The comparison process tests the equivalency of true labels and derived classifications to generate an epoch classification accuracy statistics report and a corresponding classification matrix representing the fraction of epochs of each true epoch type which are classified as belonging to each of the classified epoch types. High classification accuracy, on testing epochs which are separate and distinct from the training epochs used for learning, indicates a valid derived interpretation map.

3.5   Event Resolution Imaging Mathematical Methodology:

The specific mathematical methodology of ERI is as follows. Consider a general wavefield ψ (t), over time t, which may possess multiple channels, sensors, or vector components i. Suppose that associated with the wavefield ψ (t) there exists a set of meaningful events *A, B, C...* Further suppose that the events *A, B, C...* have specific times of occurrence, and that these times of occurrence may correspond with some of the times t of the wavefield ψ (t). Further suppose that there may be a meaningful relationship, correspondence, or association between a certain event A and its time of occurrence t, and a certain wavefield ψ (t)**,** and an ordered sequence of times of occurrence $t_1, t_2, ...t_n$ such that the event's time of occurrence t happens either during or near in time to an epoch ($t_1...t_n$) such that ($t_1 < t < t_n$), or t is near t_1 or t_n. This epoch ($t_1...t_n$) may be extracted from the general wavefield ψ (t) to produce a finite *segment* of the wavefield ψ^S(t). The wavefield segment ψ^A(t) corresponding to an event *A* may contain information *relating* to

the presence of the event *A*. This wavefield segment may also contain other wavefield information that may have *no relation* to the event *A*. Consider a collection of wavefield segments $\psi^A(t)$, $\psi^B(t)$, $\psi^C(t)$, ... corresponding to meaningful events *A, B, C,* ... such that the signal of interest may be small compared to the noise present (signal to noise ratio < 1). Further suppose that the physical, mathematical or statistical characteristics of the signal of interest may be unknown, arbitrarily complex, or highly uncertain. This means that either there is no known model for the signal of interest or that the complexity of the model or the uncertainty within the model is such as to render the model either partially or totally useless for practical purposes. Suppose that one wishes to know whether a particular event *E* is present, or associated with, a particular wavefield segment $\psi^S(t)$ where the event *E* is taken from the set of events of interest *A, B, C,...* Further suppose that the collection of wavefield segments may be divided into two or more subsets, and that at least one of these subsets of wavefield segments possesses *known* events.

Wavefield Segmentation:

Consider a wavefield $\psi_i(t)$ over time where *i* is a channel or vector index. Consider two events *A* and *B* that occur at times associated with the wavefield $\psi_i(t)$. We divide or partition the wavefield into a collection of segments or epochs $\{\psi_i^A(t)\}$ corresponding to event *A,* and $\{\psi_i^B(t)\}$ corresponding to event *B*:

$$\psi_i(t) \rightarrow \left\{ \psi_i^A(t) \right\}, \left\{ \psi_i^B(t) \right\} \qquad (1)$$

Feature Expansion:

Wavefield features $f_l^A(t)$ are extracted by expanding each wavefield segment $\psi_i^A(t)$, via a feature expansion operator T_{jk}. The feature expansion operator T_{jk}, may be designed to extract all features believed by an expert to possibly contain event-related information relating to the signal classification problem at hand. Features of interest may also consist of times (e.g., latencies relative to stimuli) and signal frequencies or pattern periodicities. Time and frequency features may be encoded into a time-frequency expansion operator T_{jk}. The time-frequency expansion operator T_{jk} is used to expand each wavefield segment $\psi_i^A(t)$ into a high dimensional time-frequency phase space where *j* represents the index over multiple times, *k* represents the index over multiple frequencies, and $l = \{i, j, k\}$ represents the index over channel *i*, time *j*, and frequency *k*:

$$f_l^A(t) = T_{jk} \left[\psi_i^A(t) \right] \qquad (2)$$

Feature Covariance:
A feature covariance matrix $M_{lm}{}^A$ is constructed from the wavefield features $f_l{}^A(t)$ of event type A by integrating over time t:

$$\mathbf{M}_{lm}^{A} = \int dt\, f_l^A(t)\, f_m^{*A}(t)$$

(3)

where l and m are feature indices and $*$ indicates complex conjugate.

Eigenvector Analysis:
The eigenvectors V^A and eigenvalues λ of the feature covariance matrix M^A are calculated corresponding to event A by solving equation (4). The eigenvectors V^B of the feature covariance matrix M^B are also calculated corresponding to event B:

$$M^A \left| V^A \right\rangle = \lambda \left| V^A \right\rangle$$

(4)

where standard bracket notation is used to designate vectors.

Feature Combinations:
Linear combinations of the eigenvectors V^A and V^B *are* constructed by means of a linear combination generation operator L to generate feature combinations X^{AB} of information corresponding to both events A and B:

$$X^{AB} = L\left(V^A,\ V^B \right)$$

(5)

Separation Analysis:
A discriminant subset of feature combinations Z_n^{AB} are selected by means of applying a discriminant separation operator D_c to the set of feature combinations X^{AB} according to a selection criterion c. One useful selection criterion c is to find the threshold separation value that maximizes the classification accuracy.

$$\left| Z_n^{AB} \right\rangle = D_c\left(X^{AB} \right)$$

(6)

Single-Trial Signals:
The nth single-trial signal $\varphi_n^S(t)$ is constructed by taking the inner product of the wavefield features $f^S(t)$ for epoch segment S with the nth discriminant feature combination Z_n^{AB} which has been selected to optimally distinguish epoch segments corresponding to event type A from those corresponding to event type B:

$$\varphi_n^S(t) = \left\langle f^S(t) \middle| Z_n^{AB} \right\rangle$$

(7)

Note that the single-trial signal $\varphi_n^S(t)$ is a composite waveform representing a weighted linear combination of wavefield features.

Signal Attributes:
Signal attributes $\alpha_{mn}(s)$ are constructed corresponding to attribute calculation operators F_m by integrating over the time t of epoch segment s:

$$\alpha_{mn}(s) = \int dt \; F_m\left[\varphi_n^S(t)\right] \qquad (8)$$

Event Probability:
The signal attributes $\alpha_{mn}(s)$ are used to calculate the probability that the epoch segment s is associated with event A by means of an attribute selection and probability normalization operator N:

$$P(s) = N\left[\alpha_{mn}(s)\right] \qquad (9)$$

Epoch Classification:
The event probability $P(s)$ and a classification function C are used to calculate the crisp classification $E(s)$ of epoch segment s:

$$E(s) = C\left[P(s)\right] \qquad (10)$$

The epoch classification $E(s)$ will be either event type $E(s) = A$ or event type $E(s) = B$. For truth state evaluations, these crisp epoch classifications correspond to definitions of either truth *state A (non-deception) or truth state B (deception)*.

For ERI analysis, 400 epochs (25 sec/epoch) were extracted from the PDD data, at the onset of various deceptive and non-deceptive questions. These epochs were chosen in order to provide the software's learning algorithm with a balanced representation of both states. These two sets of deceptive and non-deceptive data were then divided, each consisting of 400 epochs into two sets each: a learn set and a classify set. The learn set was made up of 300 epochs and the classify set was made up of 100 epochs. There were several maps created to analyze this data. These maps differed only in the times and frequencies and channels that were selected by the user. The fact that two sets were used a constraint on the total number of epochs needed: fewer epochs in the learn set yielded lower learn-generality (and therefore lower accuracies in the classify process), and fewer epochs in the classify set would yield lower certainty. No overlapping was allowed in the selection of epochs, to promote generality in the learned model, and to yield higher statistical confidence in the discrimination accuracy. Discrimination accuracy is defined as the total number of correctly classified epochs divided by the total number of epochs. Similarity is calculated from accuracy by the following formula: $S = 1 - 2A$, where A is the discrimination accuracy and S is the similarity.

3.6   Other Data and Statistical Analyses:

1. The *three point features* that were found by other researchers to yield the best results for the automated scoring of Zone Comparison Test exams were initially evaluated. These point features are as follows:

   a. *Amplitude of the Electrodermal Response*: This is the amplitude of the EDR rise following the question onset.

   b. *Total Length of the Respiration Waveform:* This is the total line length of the combined respiratory traces following question onset. This combined line length of the respiratory waveforms captures decreases in both respiratory frequency and respiratory amplitude.

   c. *Amplitude of the Baseline of the Cardiovascular Waveform:* This is the amplitude of the baseline, or lower envelope, of the cardiovascular trace following question onset.

The point features were then processed by the ERI process as described in section 3.4.

The processing shown in Figure 4 is described as follows:

   a. Multiple interpretation maps were used to classify a subject using the ERI process.

   b. Activation value plots generated for this subject using the interpretation maps were collapsed into several histograms (one histogram for each activation value plot).

   c. From the processed data created in 'b', a new interpretation map was generated (again using the ERI process with different settings).

   d. This new interpretation map was used to classify the blind subjects which yielded a single activation value for each subject (see **Figure 4**).

If the single activation value for each subject was positive, then the subject was presumed to be truthful for all R3 questions. If the single activation value for each subject was negative, then the subject was assumed to be deceptive to all R3 questions. This is how the final decision of truth or deception for each of the unknown subjects was determined.
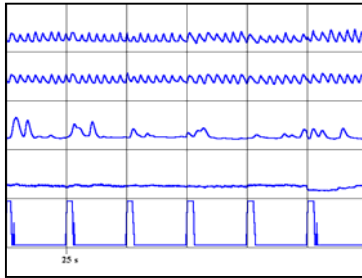
FIGURE 4
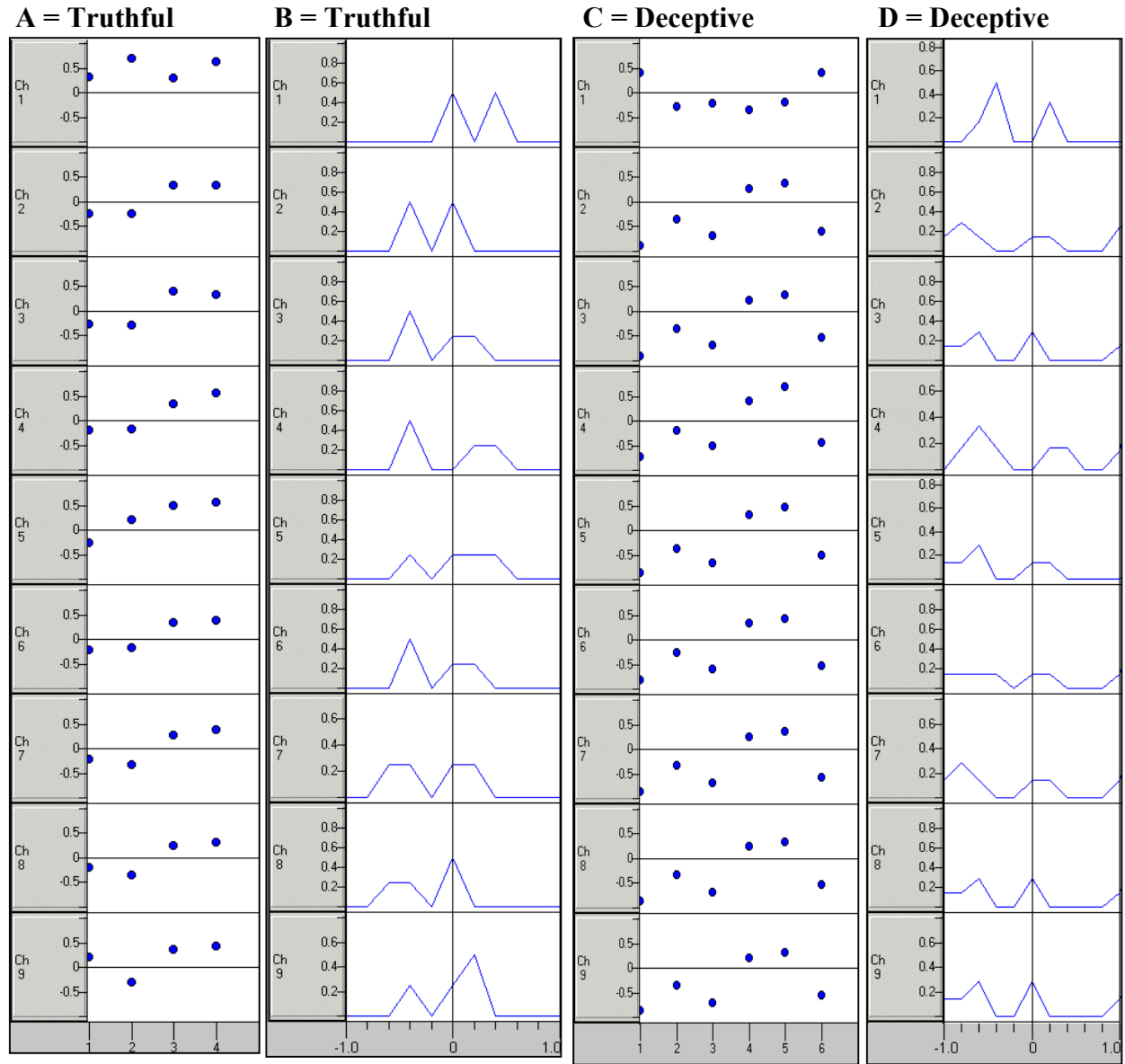
Figure 4. Single Subject Histogram: Figures 4A and 4C show the results of ERI processing on 2 subjects (1 deceptive and 1 truthful), where each activation value represents an epoch of PDD waves (time-locked to the beginning of the R3 question). These values range between 1.0 and −1.0 (as shown on the y-axis), with those that are positive assumed to be truthful and those that are negative assumed to be deceptive. Each dot on the x-axis indicates a subject's response.

Figures 4B and 4D show the histogram that was created for each respective subject. Each spike in the histogram represents one or more questions. The height of the spike represents the number of questions that fell at that point on the activation value plot. The y-axis indicates a subject's response. The x-axis is labeled from −1.0 to 1.0 and represents the activation space.

FIGURE 5
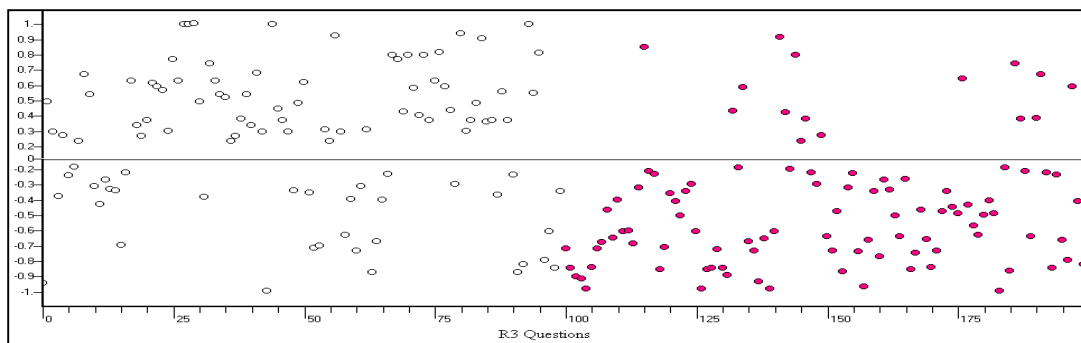
A **Truthful PDD Wave Patterns**   B   **Deceptive PDD Wave Patterns**
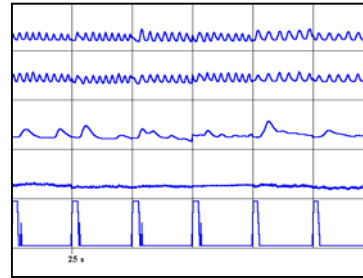
C   **Single Response Plot**
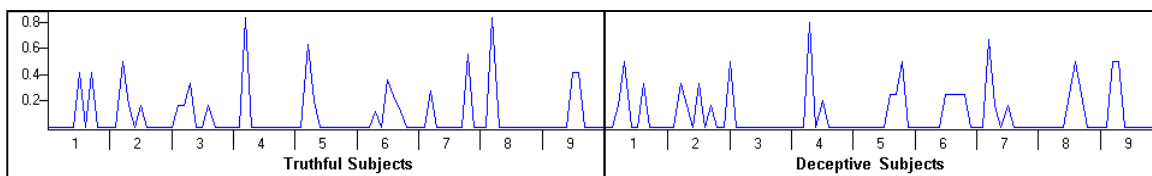
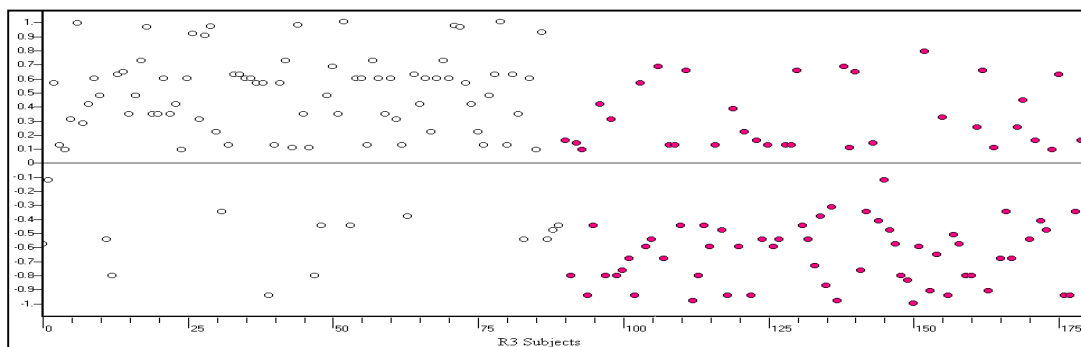D   ○ = Truthful Responses   ● = Deceptive Responses

Response Histograms for Multiple Subjects

E   **Individual Subject Plot**

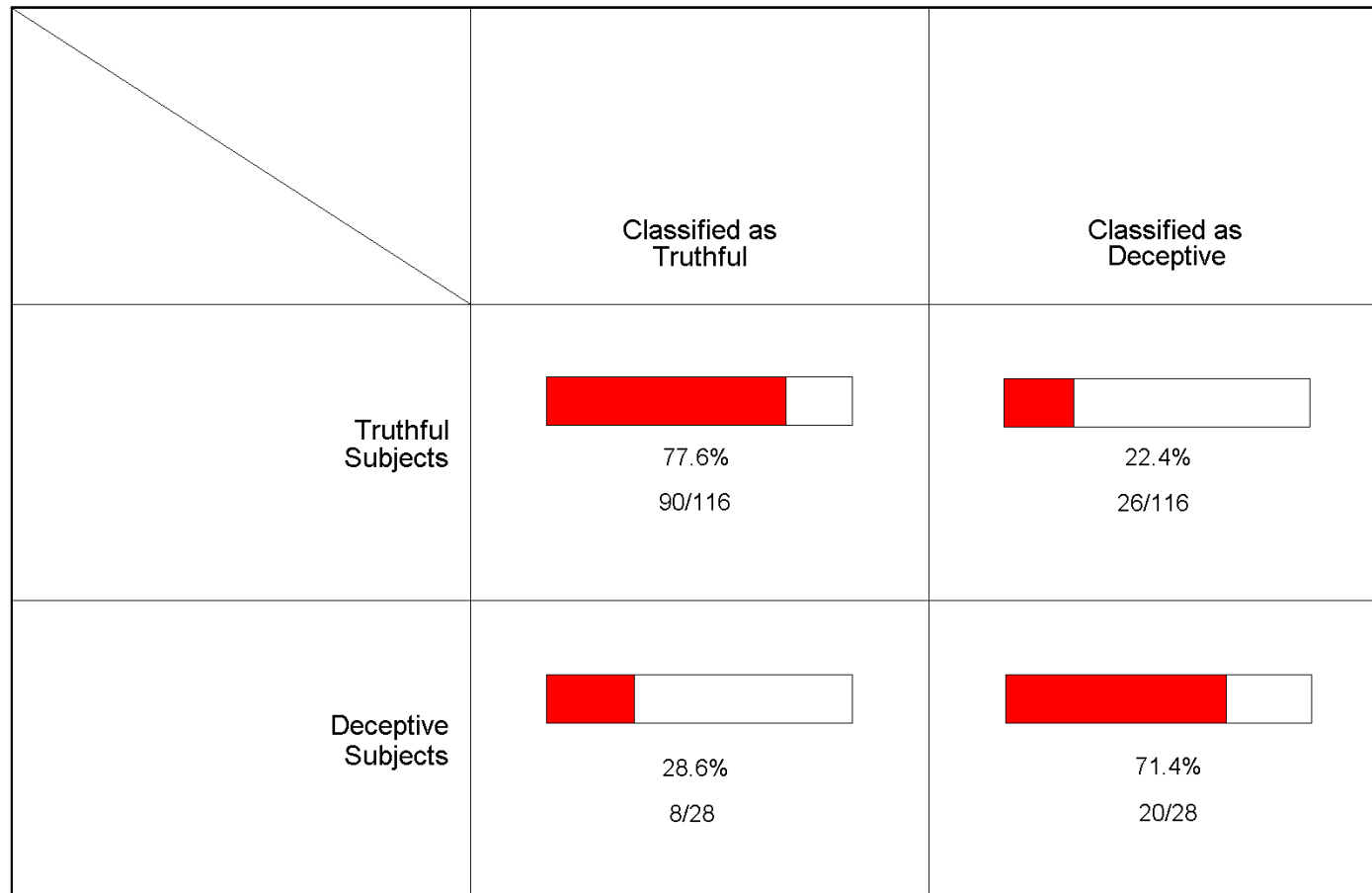○ = Truthful Subjects   ● = Deceptive Subjects

21

Figure 5. Summary of Process: This figure outlines the process used for this study. **Figures 5A and 5B** depict the raw PDD waves as displayed in the software. The waves in **Figure 5A** are from a truthful subject, and the waves in **Figure 5B** are from a deceptive subject. Notice that it is difficult to discern between these waves with the naked eye. **Figure 5C** shows a PDD activation value plot for a set of truthful vs. deceptive R3 questions. Each activation value represents a subject's response to an R3 question, which has been processed using the Event Resolution Imaging (ERI) technique developed by Thoughtform. In **Figure 5C** there are 3-5 activation values per subject, which range between 1.0 and −1.0 on the y-axis. The range of the activation value point on the y-axis represents the degree of truthfulness or deception for a particular question. The closer to 1.0 the more truthful that question is believed to be. The x-axis depicts the total number of responses therefore each increment on the x-axis is an individual response to a question. These activation values were collapsed into a single epoch to create a histogram for each of the subjects (**Figure 5D**). A spike in the histogram represents an activation value point for one of the R3 questions for that subject. The subject's histogram was then subjected to the ERI process to give an assessment of whether the subject was truthful or deceptive. This process was repeated for each subject. In **Figure 5E**, one activation point represents one subject's histogram, after having been processed using the ERI technique. The range of the activation value point on the y-axis represents the degree of truthfulness or deception for a particular subject. The closer to 1.0 the more truthful that subject is believed to be. The x-axis depicts the total number of subjects therefore, each increment on the x-axis is an individual subject. Running the ERI process on the histogram for each subject was found to be more accurate than averaging and gave the final classification for each subject with regards to the R3 question.

4.0   RESULTS

Using the detailed protocol described above, an R3 classification of the 144 blind or mystery subjects has been constructed for this R/I polygraph research project. In this classification, we have removed the clearing charts from the 144 mystery subjects.   However, the clearing charts were not removed from the 577 visible subjects, which were used for learning.

The computerized analysis technique described above has been used in a true blind test involving 144 blind subjects. The three-column chart of classifications in appendix 1 was sent to the Department of Defense Polygraph Institute on October 19, 2001. It was determined that the computerized analysis technique described in this final report correctly identified 20 of the 28 (71.4%) subjects who were deceptive to relevant question #3 (Have you used any marijuana during the last 30 days?), and 90 of the 116 (77.6%) subjects who were truthful to relevant question #3 for an overall accuracy rate of 76.4% on the 144 blind subject as illustrated in **Figure 6**.   According to a personal communication from the DoDPI one of the leading commercial scoring algorithms obtained an accuracy of 63.2% on the same data set. The DoDPI has pilot data that suggests that human scorers of multiple-issue R/I screening examinations perform at approximately 70% accuracy for dichotomous decisions.   Therefore, this new computerized analysis method demonstrated that it can produce a higher scoring accuracy than that obtainable by human experts, as well as outperform other commercial scoring algorithms.

FIGURE 6

**Figure 6. Classification Accuracy Matrix:** Illustrates the accuracy for this study. Of the 116 truthful subjects, 77.6% were classified correctly and 22.4% were classified incorrectly. Of the 28 deceptive subjects, 71.4% were classified correctly and 28.6% were classified incorrectly. See Appendix 1 for a complete classification of each subject with the activation that each subject received.

FIGURE 7
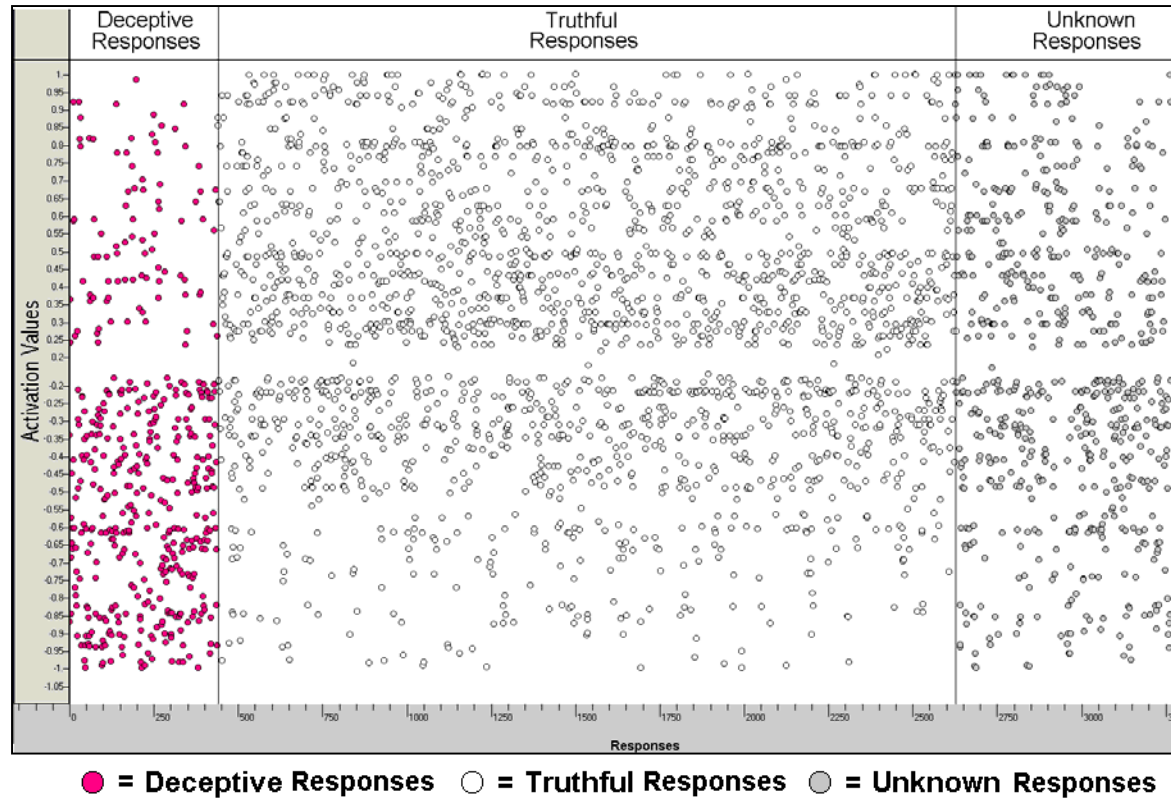
Figure 7. PDD Activation Value Plot for Individual R3 Questions: Illustrates a PDD Activation Value Plot that includes all of the R3 questions that were supplied by the DoDPI. The range of the activation value point on the y-axis represents the degree of truthfulness or deception for a particular R3 question. The closer the activation value point is to 1.0, the more truthful that question appears to be. The closer the activation value point is to –1.0, the more deceptive that question appears to be. The x-axis depicts the total number of questions. Therefore, each increment on the x-axis is an individual question. The activation values in front of the first line are the R3 questions which were responded to deceptively. The activation values in front of the second line represent the R3 questions which were responded to truthfully. The activation values following the second line are the responses to the R3 questions for which the ground truth was withheld. There were 450 deceptive responses to question R3, 2181 truthful responses, and 641 responses for which the response veracity was unknown.

24
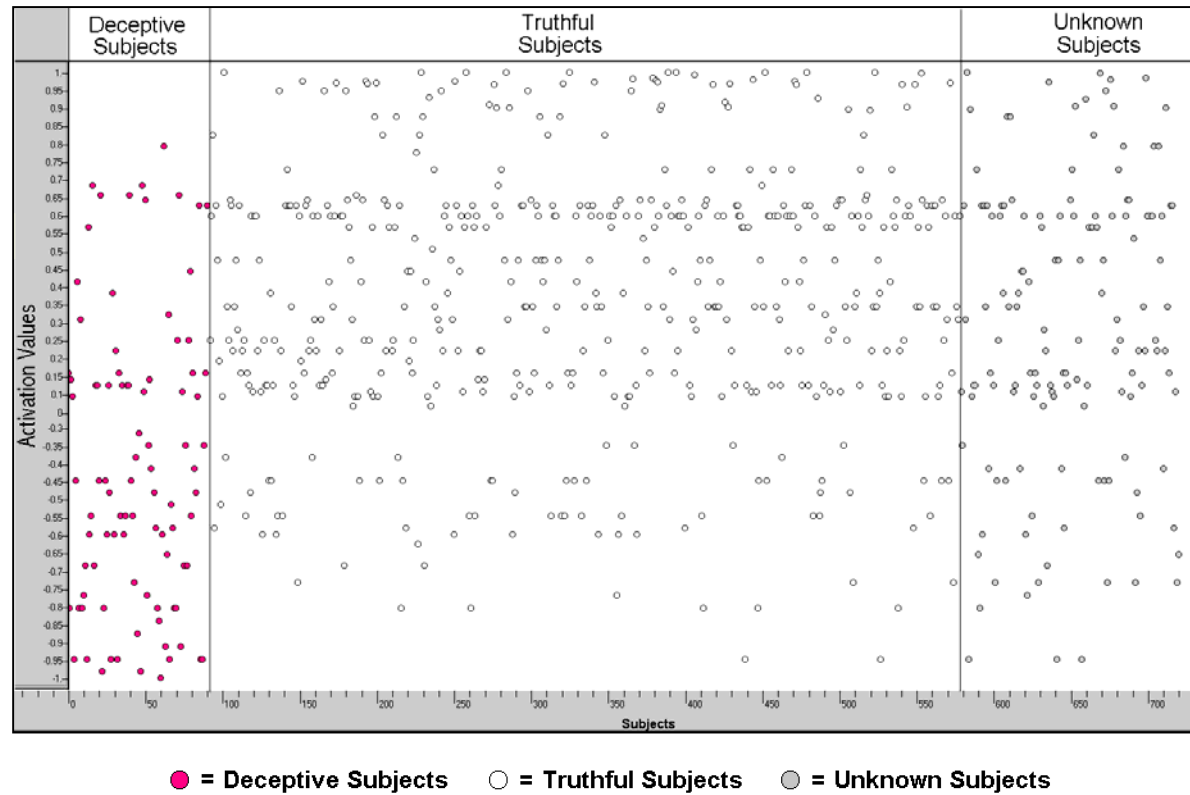
FIGURE 8

Figure 8 PDD Activation Value Plot for Deceptive and Truthful R3 Subjects shows a PDD Activation Value Plot that includes all of the subjects that were supplied by the DoDPI. Each activation value represents one subject's histogram as shown in Figure 5D. The range of the activation value point on the y-axis represents the degree of truthfulness or deception for a particular subject. The closer to 1.0 the activation value point is the more truthful that subject appears to be. The closer to −1.0 the activation value point is the more deceptive that subject appears to be. The x-axis depicts the total number of subjects therefore, each increment on the x-axis is an individual subject. The activation values in front of the first line are the subjects which were deceptive. The activation values in front of the second line are the subjects which were truthful. The activation values following the second line are the subjects for which the ground truth was withheld from the data analysts. There were 94 subjects that were deceptive to the R3 question, 483 subjects that were truthful to the R3 question, and 144 subjects whose veracity was unknown to the data analysts.

5.0 DISCUSSION

Event Resolution Imaging, which uses advanced proprietary mathematical modeling to develop signal features by simultaneously evaluating data in the time, space, frequency, and phase domains, was used to develop a system for discriminating the veracity of examinees taking a relevant/irrelevant question format polygraph examination. A model was developed which predicted examinee veracity with 80% accuracy on a pseudo-blind study using a subsample of known data. An overall veracity discrimination accuracy of 76% was subsequently obtained on a previously unexamined cross-validation sample of 144 examinations on which the ground truth was withheld.

The great advantage of these new algorithms is their use of signal features, instead of point features, as a primary method. A point feature is a feature that has been reduced to a single numerical value prior to its introduction to the scoring algorithm. For example, the value of the Total Respiration Length might be 12.39 units, so the value of this feature would be the single number 12.39. On the other hand, *signal features* have not yet been reduced, or collapsed, to a single numerical value; a signal feature still exists as an ordered collection of values. One example would be the temporally ordered collection of values that constitute the baseline waveform of the cardiovascular trace. In such a case, a signal feature may be viewed as an ordered collection of point feature values (such as 4.32, 4.38, 4.43, 4.41, 4.35…) or as a feature that is an entire waveform rather than just a single numerical value derived from the waveform. In other words, a signal feature is a whole signal, not just a point.

In the field of Electroencephalography (EEG) and Evoked Potential (EP) research, the benefit of employing signal features rather than point features is enormous. The use of signal features in EEG has yielded high-quality single-trial evoked potentials and high-accuracy single-trial event classification capabilities which were never achieved prior to the introduction of signal features.

Signal features were evaluated that represent *well-known physiological phenomena* including *frequencies, response latencies, phase relationships amplitudes* and:

1. Electrodermal Response including electrodermal response latencies and amplitudes.

2. Thoracic and Abdominal Respiratory frequencies, baseline amplitudes, and response latencies.

3. Cardiovascular frequencies, baseline amplitudes, and response latencies.

4. Correlations among thoracic and abdominal respiratory frequencies, phases, amplitudes and latencies.

5. Correlations between cardiovascular and respiratory frequencies, phases, baselines and latencies. These correlated signal features will provide useful insight into relationships such as how the frequency of respiration changes with the cardiovascular baseline.

6. Correlations between the electrodermal response and the frequencies, phases, baselines, amplitudes and latencies of the cardiovascular and respiratory responses.

In summary, a broad selection of signal features were evaluated to explore correlations and inter-channel relationships among the amplitudes, baselines, frequencies, phases, and latencies of the electrodermal response, thoracic respiration, abdominal respiration and cardiovascular activity.

There is significant utility in using signal features rather than point features to explore and evaluate the discrimination potential of inter-channel relationships and inter-feature correlations. A signal feature simply contains *more information* than a point feature. A point feature consists of just a single value of information, whereas a signal feature possesses a whole string of information values. The rich information content of signal features provides more useful and meaningful correlations between distinct physiology channels.

For example, it is possible to extract phase-encoded information by correlating the occurrence of a particular frequency of one channel with a distinct frequency of another channel. Also, a baseline amplitude change may concur with a latency shift or phase shift in a separate channel. Some of these correlations, even those which are difficult to observe in raw physiological traces, may be relatively robust and indicative of deception. The use of signal features may therefore reveal useful physiological correlations that have been relatively obscure due to the complexity of raw physiological signals.

To improve upon this study in the future, it would be beneficial to utilize a larger database for the refinement of current algorithms. Algorithms could be applied more generally towards other questions and other types of tests. This would be helpful in the field to support polygraph examiners.

Another problem encountered while analyzing the data was clearing charts in the data. After having questioned the examinee, the polygraph examiner confronted the examinee about his response to a question that the examiner feels is deceptive based on the physiological signals, thus giving the examinee a chance to change his answer. When the examinee changes his answer, the examiner will run a chart again to view the change in the physiological signal. This chart is called a clearing chart. The response had changed, and so the physiology based on that response changed as well. That is why these charts were to be removed. In this study, however, the existence of these charts was unknown until the interpretation maps had already been created. The software had used these charts and their data to create the maps, but the charts were removed from the unknown subjects before they were assessed. Had the clearing charts been properly removed from the data prior to creating the algorithms, a higher accuracy would have been more likely attained.

In conclusion, this pilot study has been a success because scoring algorithms have been developed that can effectively distinguish deceptive subjects from non-deceptive subjects. In the future, a larger database and the early removal of clearing charts would improve application and results. Based upon the results of this pilot study, it would be very beneficial to continue work in the area of developing a generalized computer scoring algorithm for the Relevant/Irrelevant format of the Physiological Detection of Deception.

7.0   REFERENCES

Abrams, S. (1989). *The Complete Polygraph Handbook,* Lexington, Massachusetts/Toronto: Lexington Books.

Achim, A., & Marcantoni, W. (1997). Principal component analysis of event-related potentials: Misallocation of variance revisited. *Psychophysiology*, 34, 597-606.

Applied Physics Laboratory, Johns Hopkins University, "Polygraph Automated Scoring System User's Guide, Version 2.1," 1993. This research was contracted by the NSA.

Axciton, produced and distributed by Axciton Systems, Inc., P.O. Box 42380, Houston, Texas 77242. This development was partially funded under a federal grant contract.

Bertrand, J., et. al. (1994). Time-frequency filtering based on an invertible wavelet transform: An application to evoked potentials, IEEE Trans. *Biomedical Engineering*, Vol. 41, No. 1, (pp. 77-88).

Buchner, H., et. al. (1994). Preoperative localization of the central sulcus by dipole source analysis of early somatosensory evoked potentials and three-dimensional magnetic resonance imaging. *Journal of Neurosurgery*, 80, 849-856.

Burch, N. R. (1969). Online Classification of Polygraph Responses, *Final Report*, Department of the Navy, Office of Naval Research, Washington, D.C., Contract N00014-67-C-0493, October, 1969.

Cardenas, V. A., et. al. (1995). A multi-channel, model-free method for estimation of event-related potential amplitudes and its comparison with dipole source localization. *Journal of Medical Engineering and Technology*, 19, 88-89.

Carpenter, G. A., & Grossberg, S. (1991). *Pattern Recognition by Self-Organizing Neural Networks*, London: The MIT Press.

Chapman, R. M., & McCrary, J. W. (1995). EP component identification and measurement by principal component analysis. *Brain and Cognition*, 27, 288-310.

Computerized Polygraph System, produced and distributed by Stoelting, Oakwood Center, 620 Wheat Lane, Wooddale, Illinois 60191. The CPS development and the CAPS were partially funded by the United States Secret Service (USSS) and another federal agency.

Cook, D. R., et. al. (1993). Phase-space action conservation for non-eikonal wave fields. *Physics Letters*, A174, 53.

Cook, D. R., et. al. (2001). Polygraph Decision Support System for Relevant / Irrelevant Format Examinations. *In preparation. To be submitted to the International Journal of Psychophysiology in Fall 2002.*

Cook, D. R., et. al. (2001). Single-Trial Somatosensory Evoked Signals. *Submitted to the International Journal of Psychophysiology in May 2001.*

Cook, N. S., et. al. (2001). Single-Trial Visual Evoked Signals. *Submitted to the Journal of Clinical Neurophysiology in May 2001.*

Cook, N. S., et. al. Few-trial Cognitive Event Related P300 Electroencephalographic signals. *In Preparation. To be submitted to the Journal of Clinical Neurophysiology in 2002.*

Ebersole, J. S. (1991). EEG dipole modeling in complex partial epilepsy. *Brain Topography*, 4(2), 113-123.

Fuchs, M., et. al. (1995). "Cortical current imaging by morphologically constrained reconstructions". Biomagnetism: *Fundamental Research and Clinical Applications*, C. Baumgartner et al. (Eds.), (pp. 320-325). Elsevier: Science IOS Press.

Golub, G. H., & Van Loan, C. F. (1989). *Matrix Computations*, London: The John Hopkins University Press.

Giles, F. and Yankee, W., (1986) Interfaced with CODAS software with a Stoelting Polygraph and collected real time physiological data during an analog study by Yankee, William and Giles, Fred, "A Comparison Between Control Questions and Relevant-Irrelevant Polygraph Test Formats in a Screening Situation." Final Report MDA 904-86-R-2192.

Haykin, S. (1991). *Adaptive Filter Theory*, New Jersey: Prentice-Hall.

Honts, C. R. (1986). Countermeasures and the Physiological Detection of Deception: A Psychophysiological Analysis, Unpublished doctoral dissertation, University of Utah, 1986.

Horn, R. A., & Johnson, C. R. (1985). *Matrix Analysis*, New York: Cambridge University Press.

Ingber, L. (1995). Statistical mechanics of multiple scales of neocortical interactions in: P. L. Nunez, Neocortical Dynamics and Human EEG Rhythms. *Oxford University Press*, New York, (pp. 628-681).

James, E. (1982). produced and distributed a program for the VIG 20 Commodore computer and later for the Commodore 64, to provide "…computer assisted chart evaluation," published 1982.

Kircher, J. and Raskin, D. (1988). Human Vs. Computerized Evaluations of Polygraph Data in a Laboratory Setting, *Journal of Applied Psychology*, Vol. 73, No. 2, 1988, pp. 291-302.

Kircher, J. C. and Raskin, D. C. (1989). *Computer-Assisted Polygraph System, Version 6.00 and 6.01 User's Manual,* Scientific Assessments Technologies, Inc., 1865 Herbert Avenue, Salt Lake City, Utah, 1989.

Kosko, B. (1992). *Neural Networks for Signal Processing*, New Jersey: Prentice-Hall.

Kosko, B. (1992). *Neural Networks and Fuzzy Systems*, New Jersey: Prentice-Hall.

Kubis, J. F. (1962). Studies in Lie Detection, Fordham University, New York, NY, AF30 (602)-2270, Project No. 5534, Task No. 553401, 1962.

Lafayette LX-2000-101 and 105, produced and distributed by Lafayette Instruments, 3700 Sagamore Parkway North, P.O. Box 5729, Lafayette, Indiana 47903. This system was preceded by another computerized polygraph system and was partially funded by a federal agency.

Makeig, S. (1993). Auditory event-related dynamics of the EEG spectrum and effects of exposure to tones. *Electroencephalography and Clinical Neurophysiology*, 86(4), 283-293.

McGuigan, F. J. and Pavek, G. U. (1972). On the Psychophysiological Identification of Covert Non-Oral Language Processes, *Journal of Experimental Psychology*, Vol. 92, No. 2, 1972, pp. 237-245.

Nunez, P. L. (1986). Locating sources of the brain's electric and magnetic fields: Some effects of inhomogeneity and multiple sources, with implications for the future. *Human Factors and Organizational Systems Laboratory Technical Note 71-86-12*, US Navy San Diego.

Nunez, P. L. (1988). Spatial filtering and experimental strategies in EEG. In: D. Samson-Dollfus (Ed.), *Functional Brain Imaging,* (pp. 196-209). Paris: Elsevier.

Podlesny, J. A. (1976). Effectiveness of Techniques and Physiological Measures in the Detection of Deception, *Dissertation*, University of Utah, 1976.

Raskin, D., Kircher, J., Honts, C., Horowitz, S. (1988). A Study of the Validity of Polygraph Examinations in Criminal Investigations*, Final Report to the National Institute of Justice*, Grant No. 85-IJ-CK-0040, May, 1988.

Scherg, M. (1990). Fundamentals of dipole source potential analysis. Auditory evoked magnetic fields and electric potentials. In F. Grandori, M. Hoke, & G. L. Romani (Eds.), *Advances in Audiology*, 6, 40-69.

Scherg, M. (1992). Functional imaging and localization of electromagnetic brain activity. *Brain Topography*, 2(5), 103-111.

Scherg, M., & Berg, P. (1991). Use of prior knowledge in brain electromagnetic source analysis. *Brain Topography*, 4(2), 143-150.

Scherg, M., & Ebersole, J. S. (1993). Models of brain sources. *Brain Topography*, 4(5), 419-423.

Scherg, M., et. al. (1989). Frequency-specific sources of the auditory N19-P30-P50 response detected by a multiple source analysis of evoked magnetic fields and potentials. In: S. J. Williamson, et al. (Eds.). (pp. 97-100). New York: Plenum Publishing Corporation.

Short R. M., et. al. (2002) Classification of motor evoked electroencephalographic signals. *In preparation. To be submitted to the International Journal of Psychophysiology in 2002.*

Steffensen, S. C., et. al. (2001) A Novel Electroencephalographic Analysis Method Discriminates Alcohol Effects from those of other Sedative/Hypnotics. *Submitted to the Journal of Neuroscience Methods in May 2001.*

Thoughtform Interpretation Studio Copyright © Thoughtform Corporation 1998-2001, Versions 1.0, 1.1, 1.2, 2.0, 2.1, 2.2, 3.0, developed, produced and distributed by Thoughtform Corporation, 85 West 400 North, Bountiful, Utah 84010, (800) 854-5272, (801) 299-1285.

Timm, H. W. (1989). Methodological Considerations Affecting the Utility of Incorporating Innocent Subjects into the Design of Guilty Knowledge Polygraph Experiments, *Polygraph*, Vol. 18, No. 3, pp. 143-157.

Turetsky, B., et. al. (1990). Representation of multi-channel evoked potential data using a dipole component model of intracranial generators: Application to the auditory P300. *Electroencephalography and Clinical Neurophysiology*, 76, 540-556.

Witte, H., et. al. (1990). Using discrete Hilbert transformation to realize a general mathematical basis for dynamic EEG mapping. A methodical investigation. *Automedica*, 13, 1-13.

Wood, C. C., & McCarthy, G. (1984). Principal component analysis of event-related potentials: Stimulation studies demonstrate misallocation of variance across components. *Electroencephalography and Clinical Neurophysiology*, 59, 249-260.

Yankee, W. J. (1968). A Report on the Computerization of Polygraphic Recordings, Presented to the Fifth Annual Seminar of the Keeler Alumni Association, July, 1968.

Yankee, W. J. (1995). The Current Status of Research in Forensic Psychophysiology and its Application in the psychophysiological Detection of Deception, *Journal of Forensic Sciences*, JFSCA, Vol. 40, No. 1, January 1995, pp. 63-68.

Zhang, Z., & Jewett, D. L. (1993). Insidious errors in dipole localization parameters at a single time point due to model misspecification of number of shells. *Electroencephalography and Clinical Neurophysiology*, 88, 1-11.

Zhang, Z., et. al. (1994). Insidious errors in dipole parameters due to shell model misspecification using multiple item points. *Brain Topography*, 6, 283-298.

APPENDIX 1: Individual Subject Classification

The chart below contains three columns. The first column is the Subject Number assigned by the researchers. In the second column, all subjects were classified as being either truthful (T) or deceptive (D). In the third column, we report the activation values generated by the ERI process.

Subject #	All Subjects Classified for R3	Activation Value for R3
1	T	0.36
2	T	0.92
3	T	0.76
4	D	-0.55
5	D	-0.31
6	T	0.2
7	D	-0.31
8	D	-1
9	T	0.24
10	T	0.51
11	T	0.65
12	T	0.33
13	T	0.92
14	D	-0.92
15	D	-0.75
16	T	1
17	T	0.3
18	D	-0.46
19	T	0.44
20	T	1
21	T	1
22	T	0.8
23	T	1
24	T	1
25	D	-0.96
26	D	-0.84
27	T	0.92
28	T	0.76
29	D	-0.65
30	T	0.33
31	T	0.65
32	T	0.07
33	T	0.27
34	D	-0.55
35	T	0.65
36	T	0.09
37	T	0.79
38	T	0.92

39	T	0.76
40	T	1
41	T	0.27
42	T	1
43	T	0.27
44	T	0.15
45	T	0.62
46	D	-0.7
47	T	0.75
48	D	-0.7
49	T	0.33
50	T	0.8
51	T	0.12
52	T	0.36
53	D	-1
54	D	-0.41
55	D	-0.31
56	T	0.8
57	T	1
58	T	0.51
59	D	-0.46
60	D	-0.12
61	T	0.92
62	D	-0.31
63	T	0.65
64	T	0.12
65	D	-0.51
66	T	0.36
67	T	0.09
68	T	0.27
69	T	0.27
70	T	0.12
71	T	0.07
72	T	1
73	T	0.65
74	T	0.27
75	T	0.65
76	T	1
77	T	0.94
78	T	1
79	T	0.33
80	T	0.59
81	D	-1
82	D	-0.6
83	D	-0.65
84	T	0.76
85	T	1
86	T	0.09
87	T	1
88	D	-0.6
89	T	1
90	D	-0.55
91	T	0.27
92	D	-0.6
93	T	0.17

94	T	0.33
95	T	0.07
96	T	0.12
97	T	0.27
98	D	-0.31
99	T	0.51
100	T	0.5
101	T	0.12
102	T	1
103	D	-0.55
104	D	-0.75
105	T	0.2
106	T	0.27
107	T	0.51
108	T	1
109	D	-0.55
110	D	-0.6
111	T	0.09
112	D	-0.65
113	T	0.33
114	D	-0.36
115	T	0.07
116	D	-0.7
117	D	-0.7
118	T	0.92
119	D	-0.7
120	D	-1
121	T	0.79
122	T	0.77
123	D	-0.65
124	T	1
125	D	-0.6
126	T	0.12
127	T	0.07
128	T	0.12
129	D	-0.6
130	T	0.51
131	T	0.09
132	T	0.47
133	D	-0.12
134	D	-0.55
135	T	0.44
136	D	-0.6
137	D	-0.51
138	T	0.15
139	T	0.17
140	T	0.15
141	T	0.09
142	D	-0.31
143	D	-0.65
144	T	0.36